



Installation of solar chromospheric telescope at the Indian Astronomical Observatory, Merak

B. RAVINDRA*, PRABHU KESAVAN, K. C. THULASIDHAREN, M. RAJALINGAM, K. SAGAYANATHAN, P. U. KAMATH, NAMGYAL DORJEY, ANGCHUK DORJEE, P. M. M. KEMKAR, TSEWANG DORJAI and RAVINDER K. BANYAL

Indian Institute of Astrophysics, II Block, Koramangala, Bengaluru 560 034, India.

*Corresponding author. E-mail: ravindra@iiap.res.in

MS received 31 May 2018; accepted 6 August 2018; published online 27 September 2018

Abstract. We report the observations of the solar chromosphere from a newly commissioned solar telescope at the incursion site near Pangong Tso lake in Merak (Leh/Ladakh). This new H_{α} telescope at the Merak site is identical to the Kodaikanal H_{α} telescope. The telescope was installed in the month of August 2017 at the Merak site. The telescope consists of a 20-cm doublet lens with additional re-imaging optics. A Lyot filter with 0.5 Å passband isolates the Balmer line of the hydrogen spectra to make the observations of the solar chromosphere. The observations made in H_{α} wavelength delineates the magnetic field directions at the sunspot and the quiet regions. A CCD detector records the images of the chromosphere with a pixel resolution of 0.27'' and covers 9.2' field-of-view. This telescope has a good guiding system that keeps the FoV in the intended position. We report the development of control software for tuning the filter unit, control detector system, observations and calibration of the data to make it useful for the scientific community. Some preliminary results obtained from the Merak H_{α} telescope are also presented. This high altitude facility is a timely addition to regularly obtain H_{α} images around the globe.

Keywords. Sun: chromosphere—Sun: H_{α} telescope—Sun: H_{α} surge.

1. Introduction

In 1889, George Ellery Hale built his own spectroheliograph to make a map of the Sun in a particular wavelength (Hale & Ellerman 1906). Since then, several observatories around the world have built slit-based spectroheliographs which have entrance and exit slits. The exit slit decides the pass-band of the spectroheliograph. Later, many observatories started using the filter based spectral isolators to image the Sun, particularly the solar chromosphere. Using these instruments, observatories have made full-disk Ca-K and H_{α} images recorded in the photographic plates (Srivastava *et al.* 1991; Zirin *et al.* 1982). With the advancement in the detector technology, many have started utilizing the electronic-based detectors which are more sensitive to light and obtained more uniform images (Verma *et al.* 1997; Denker *et al.* 1999; Otruba & Potzi 2003).

The H_{α} data shows the conditions of the chromosphere during the flare events. This is the best wavelength region to observe the solar flare ribbons

from ground-based observatories. The observations made in H_{α} wavelength shows the fibrillar structures which delineates the magnetic fields (Woodard & Chae 1999). The filament eruption, pre-flare brightening, rotation of prominences before the eruption, dynamics of spicules and many more interesting features could be seen in this wavelength. Mass motions inside the filaments and rotations of the prominences are studied in several cases during its eruption (Zirker *et al.* 1998; Lin *et al.* 2003; Labrosse *et al.* 2010; Mackay *et al.* 2010). With the high-resolution and long hours of observations of the filaments/prominences, it is easy to study their properties using H_{α} observations leading up to the eruption. During the flare, at the chromospheric level, two ribbons are seen which move away from each other at certain speed (Vemareddy *et al.* 2012). The identification of newly brightened pixels can be done using H_{α} wavelength. These newly brightened pixels along with the corresponding locations in the magnetograms can be used to compute the magnetic flux swept-up by the ribbons as they move apart in the chromosphere

(Qiu *et al.* 2004) and can be used to infer the reconnection rate inside the reconnecting region. The details of various other cases that can be studied with the H_{α} data is reported in Ravindra *et al.* (2016).

Kodaikanal Observatory has a history of making the full-disk solar observations in white-light, Ca-K and in H_{α} wavelengths. The white-light and Ca-K observations started in 1904 and 1905 respectively. The H_{α} observations started in 1912. Both the Ca-K and H_{α} observations were discontinued in 2007 because the production of photographic plates/films stopped. Though the white-light observations using photographic plates continued till today (Ravindra *et al.* 2013). Apart from Kodaikanal, the solar observations were also carried out at Aryabhata Research Institute of Observational Sciences (ARIES) and at Udaipur Solar Observatory (USO) using 15-cm objective, starting from 1972.

To continue the long term full-disk observations of the Sun in H-alpha, Indian Institute of Astrophysics (IIA) has worked out the main optical design and configuration of the telescope. Based on the design, two identical telescopes and Lyot filters were manufactured by Nanjing Institute of Astronomical Optics and Technology (NIAOT), National Astronomical Observatories (NAO), Chinese Academy of Sciences (CAS), China. Both the telescopes were assembled and tested in NIAOT for its performance. Out of the two telescopes, one of the telescopes was installed at the Kodaikanal Observatory in October 2014 (Ravindra *et al.* 2016). The second one was installed initially at the Center for Research and Education in Science and Technology

(CREST) campus at Hosakote by our IIA team. We have carried out in-house development of the software control and tracking system of the telescope. After completion of successful testing at CREST, Hosakote, the telescope was taken to Merak for final installation, which is also the proposed site for the 2-m class National Large Solar Telescope (NLST; Hasan 2012).

In this paper, we report the installation of the second telescope, the development of telescope control software, the technique used for guiding the telescope and filter unit. We present some of the representative results and the paper concludes with the summary of the telescope installation at Merak.

2. The telescope

The telescope is installed at Merak village, in the incursion site of Pangong Tso lake. The Merak village is located about 150 km away in the S–E direction from the Leh Town of Ladakh district in Jammu and Kashmir. This is also one of the proposed sites for putting up 2-m class National Large Solar Telescope (NLST). The site survey indicated that the viewing conditions are conducive for solar observations (Hasan *et al.* 2010). To take advantage of the large water body, the telescope is installed close to the incursion site of Pongong lake.

2.1 Telescope and re-imaging optics

Figure 1 shows the picture of the telescope after installation at the incursion site. Here, the larger

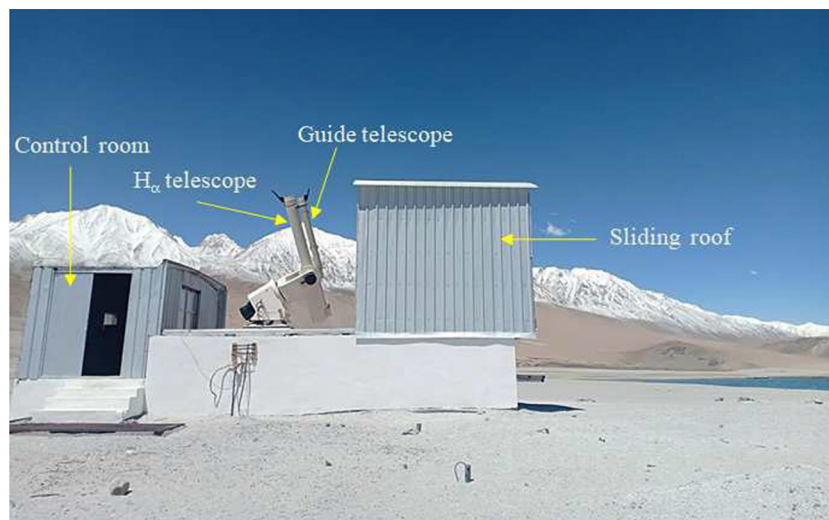


Figure 1. A picture of the H_{α} telescope making solar observations soon after the installation in August 2017. The telescope is protected by a lightweight sliding roof shown retracted in the image. Control room has the telescope electronics, power supply and computer.

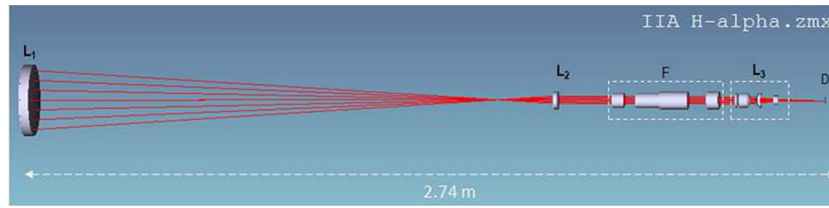


Figure 2. A schematic of the optical components and the ray diagram. In Figure, L1 is the 20 cm primary lens, L2 is the collimating lens, L3 is the refocusing lens, F is the filter unit and D is the detector position.

diameter tube is the main telescope and the smaller tube is the guide telescope. Figure 2 shows the optical layout of the main telescope designed with Zemax software. The objective lens, collimating and re-imaging optics are all enclosed inside the 3.2-m long tube of the main telescope. The objective lens is a doublet of diameter 20 cm and focal length of 158 cm. The Lyot filter is kept in between the collimator and the re-imaging setup. This forms a Sun’s image of size 2.1 cm at the focal plane. A zoom lens which can magnify the Sun’s image by 2.5 times is kept after the re-imaging lens of the main telescope. The zoom lens is motorized and it can be taken in and out of the beam path whenever required. The main usage of this lens is to make high-resolution observations of the Sun when necessary. A detailed description of the telescope and control system can be found in Ravindra *et al.* (2016).

The second smaller tube is a guide telescope. A 10-cm achromatic doublet as an objective lens which is cut into 4 pieces is fixed in a frame which holds each quadrant of the lens with a few millimeter gap in-between them. Each one of these lens produces an image at the focal plane at 4 different corners of a square with atleast 2-sides of each image overlapping with each other. The central portion of the image is dark and has a square shape with sides that are little curved. A CCD camera with 756×562 pixels is used in the focal plane to image the central dark portion. The CCD camera can accommodate only little larger than half the size of the actual image formed that includes the dark portion of the overlapped image. Figure 3 shows the central portion of the image obtained with a split lens when it is pointed towards the Sun and captured by the guide CCD camera. The detected signal is then fed into a Daheng video controller card for accessing it in computer. The image capture and analysis software is written in the Microsoft–Visual Basic platform.

The guide CCD camera is kept on X–Y linear stage which can be moved with a stepper motor. During the full-disk observations of the Sun, the dark portion falls on the center of the tube. But, during high-resolution observations, the dark portion can fall anywhere on the

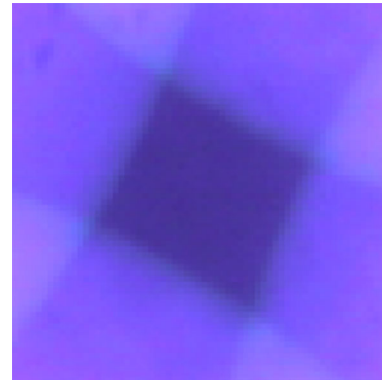


Figure 3. The image recorded by the guide CCD camera. The non-overlapping darker region in the image is used for measuring the telescope tracking errors.

circle of the tube depending on the region-of-interest. The X–Y translation stages are used to adjust the CCD positions to capture the dark portion onto the CCD camera.

An algorithm was developed to detect and track the dark portion of the image. The central dark portion of the guide image (Fig. 3) is converted into bright pixel by inverting the image. The drift in the dark portion of the image is used to find the tracking errors in RA or DEC motors. After the telescope is pointed towards the Sun, the auto guiding is enabled. The first frame is taken as the reference frame. The subsequent images grabbed thereafter is used to determine the shift in the telescope position, if any, with respect to the first frame. The inverted bright region is identified with a suitable threshold. The pixels in the dark region (inverted region) is multiplied by the corresponding intensity and then the product is summed over all the pixels. This forms the numerator and summed pixel intensity values forms the denominator. The algorithm works on the basis of finding the centroid (Prabhu *et al.* 2018) of the inverted bright region. The shift in the present image centroid is computed with respect to the reference frame centroid. The images are acquired with a cadence of one second to find the shift in the centroid. By identifying the shift in the centroid location, shift in RA and DEC axis are

Table 1. The specifications of main telescope, guider and finder telescopes.

Parts	Parameters	Values
Main telescope	Objective size	20.06 cm
	Focal length	158 cm
	Image size	2.1 cm
	Magnified image size	5.25 cm
	CCD pixels	2048 × 2048
	Pixel size (high-res)	0.27''
Guide telescope	Pixel size (low-res)	0.67''
	Objective size	10 cm
	Focal length	174.3 cm
Finder telescope	CCD pixels	756 × 562
	Objective size	3 cm
	Focal length	252.4 cm
	Image size	2.5 cm

determined. The calculated shift in both the directions are converted into Encoder counts. One pixel shift in auto guide camera corresponds to 14 encoder counts. If the shift is more than two pixels in the auto guide (28 encoder counts), then there will be a feedback sent to the control system to override the tracking, thereby correcting the error in the telescope pointing.

A small objective lens, filter and a prism makes a finder telescope which forms a 2.5 cm size image on the ground glass prism. This set-up is used during the initial stage of telescope alignment. This arrangement is also convenient to show solar images to interested public visiting the observatory.

The main telescope, guider and the finder telescope are all rigidly fixed on a common base that is attached to the equatorial fork mount whose polar axis is inclined to 33°, the latitude of the place. The telescope with pedestal is placed on a reinforced concrete pier with cast iron plate on top of the pier. The height of the pier is about 1 m and the height of the objective lens is about 4 m above the ground when the Sun is at the zenith. The mechanical structure of the telescope, direct drive motors and its specifications, break motor units, incremental encoders to get position information of the telescope etc. are all described in detail in Ravindra *et al.* (2016). The main technical parameters of the telescope are listed in Table 1.

2.2 H_{α} telescope control software

The H_{α} telescope control software was developed in the Microsoft Visual Basic platform. The drive units are controlled using National Instruments (NI) cards. The

Table 2. The specifications of the encoder unit for the RA and DEC drives at Merak H_{α} telescope.

Parameters	Value
Type of encoder	Incremental
Encoder power supply and current ratings	5 V and 250 mA
Diameter of encoder	20 cm
Number of lines	31488
Pitch width	20 μ m

necessary drivers for the NI-PCI motion controller card is installed to communicate with the servo motors of the RA and DEC drives. The telescope tracking system has two incremental encoders in RA and DEC axis respectively. The optical rotary encoders consist of a light source, rotating code disc and a light detector. The rotating code disc has graduations with equally spaced areas of dark and bright lines. As the encoder ring rotates, the light detector registers the ON-OFF pattern. The detector converts the ON-OFF pattern into a digital signal in two channels. The offset between the two channels determines the direction of the shaft rotation. The technical parameters of the RA and DEC encoders are listed in Table 2.

Each encoder has a reference position. During the initialization, the telescope moves on both axis to find the reference position or home position. From the reference position, the location of the Sun in the sky is identified using an algorithm. This algorithm was developed using the procedure given in Reda & Andreas (2008), and cross verified with the National Oceanic and Atmospheric Administration (NOAA) solar position calculation.¹ Once the telescope is pointed towards the Sun, the tracking is enabled and then the telescope starts to track the Sun at a speed of 15'' s⁻¹.

The telescope is equipped with four IR limit sensors in the four directions. In addition to this, there are four more IR sensors to monitor the limiting positions of the telescope in two directions. The use of limit sensors prevents any accidental damage to the telescope. The telescope and the filter units are controlled through Graphical User Interface (GUI) (Fig. 4).

2.3 H_{α} spectral line isolator

Solar atmosphere can be imaged by observing the Sun in isolated spectral passband. There are several ways to isolate the solar spectral line. Interference filters whose

¹https://www.esrl.noaa.gov/gmd/grad/solcalc/NOAA_Solar_Calculations_day.xls.

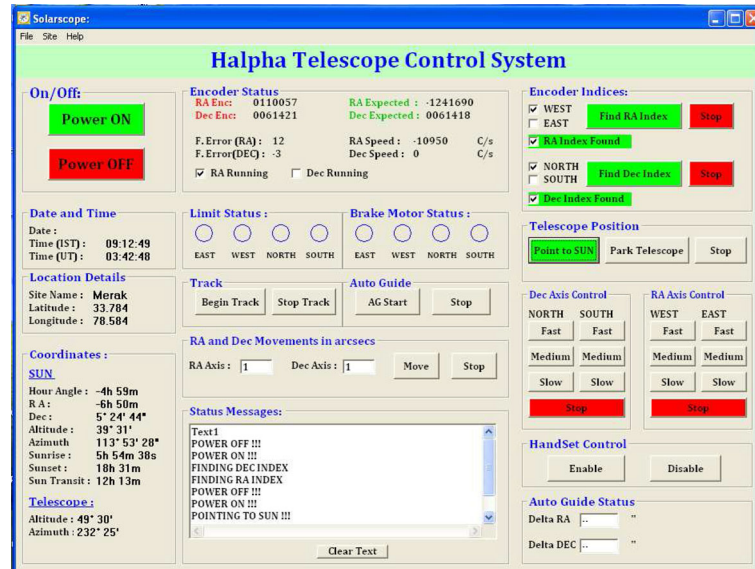


Figure 4. A screen-shot of graphical user interface developed for telescope control.

passbands of $\sim 1 \text{ \AA}$ or less is widely used to image solar chromosphere. However, the image quality is not the best due to poor contrast. Some of the observatories use mica-based Fabry–Ferrot interferometers whose passband could be anywhere between $0.4\text{--}0.6 \text{ \AA}$ (GONG; Hill *et al.* 2009). Some others used lithium niobate-based or liquid crystal variable retarders (LCVRs)-based voltage tunable filters (Tomczyk *et al.* 2016; Hagino *et al.* 2014). Birefringent crystals-based Lyot filter (Bethge *et al.* 2011), Michelson interferometer-based filter used in Michelson Doppler Imager (MDI; Scherrer *et al.* 1995) and Solar Dynamics Observatory (SDO; Scherrer *et al.* 2012) were also used. Compared to Fabry–Perot-based filters, birefringent filters have a large field-of-view but the throughput is less.

The design used in Lyot filter of H_{α} telescope installed at Merak has 7 stages of calcite crystals. The filter bandwidth is of 0.5 \AA and the free spectral range (FSR) is about 52 \AA . The whole assembly is motorized to tune the wavelength positions. The filter can be tuned as far as 4 \AA away from the line center with a spectral position accuracy of 10 m\AA . The complete filter assembly was immersed in a silicone oil chamber to ensure uniform temperature distribution. Since the refractive index of the crystals and the silicone oil almost match with each other, the use of silicone oil reduces the internal multiple reflections between the crystals at the interface. The temperature is controlled by two stage heating around different layers of the filter unit. The system can work with the ambient temperature ranging from -20°C to 35°C . A 30 \AA pre-filter is kept in front of the Lyot filter to isolate the H_{α} spectral line and reject

Table 3. The specifications of H_{α} Lyot filter existing at Merak telescope.

Parameters	Value
Central wavelength	6562.82 \AA
Passband	0.5 \AA
Free spectral range	51.2 \AA
Pre-filter passband	30 \AA
Scanning range	4 \AA on both sides from the central wavelength
Scanning step size	10 m\AA
Temperature and stability	42°C and 0.01°C
Number of stages of crystal	7
Acceptance angle	2°

all the other side bands. The entire Lyot filter assembly along with the pre-filter was kept in a collimated beam to avoid any shift in the passband due to beam convergence. The operating principle of the Lyot filter unit is explained in Stix (2002). More details about the Lyot filter used in H_{α} telescope at the Kodaikanal Observatory which is identical to the one used at Merak H_{α} telescope can be found in Ravindra *et al.* (2016). A few technical details about the Lyot filter is listed in Table 3.

2.4 The detector unit

The Charge Coupled Device (CCD) is an Apogee make (Alta series), used to record the image produced by the telescope with H_{α} filter. The camera is

2048 × 2048 pixels. The pixel size (7.5 μm) corresponds to 0.27'' in the high-resolution mode. The typical full-well capacity of the camera is 40000 electrons for this series. The CCD is front illuminated with quantum efficiency little larger than 30% at the H_α observing wavelength. The digital resolution of the camera is 16-bits and the CCD image can be read out with a clock speed ranging from 1–8 MHz. It has an interline transfer sensor with an exposure time varying from 1 ms to several minutes. The CCD can be cooled to 50°C below the ambient temperature. Usually, the day time temperature at Merak is less than 15°C and hence we expect the CCD to operate around –30°C or less. At this temperature the dark current is about 0.01 e[–] pixel^{–1} s^{–1}. The CCD is interfaced with the data acquisition system through the USB 2.0 port.

To get an image with full-well capacity, an exposure time of 400–500 ms was given. Though it is possible to take the images with 10 ms or better exposure time, the readout time is large between 0.5–4 s. Hence, the data cannot be used for speckle imaging to get diffraction limited images. Also, at this exposure time the number counts in the CCD pixels is very less. In future upgrades, we will use high speed cameras with exposure time of few millisecond to carry out such observations. The exposure time varies from morning to evening. Normally, the images were taken at a cadence of 10 s and in case of any events occurring on the Sun, the images acquired much higher cadence. The whole software was written in Python software, to get an image which not only controls the main telescope CCD camera, but also controls the Lyot filter stepper motors to move the spectral window on the H_α line profile.

3. Telescope installation and operation

The telescope was installed in the month of August 2017 at the Merak village near the Pangong Tso lake. The width of the lake is about 2 km and the length is about 130 km. The maximum depth of the water is about 100 m. The large water body near the incursion site makes the viewing better which in turn improves the image quality of the telescope.

The telescope was installed on August 30, 2017 at the Merak site. When the telescope was installed, two large sunspot groups were present on the Sun, one in the Northern (AR NOAA 12674) and another one in Southern hemisphere (AR NOAA 12673). Since the detector area is small, it is not possible to cover the full-disk of the Sun in any mode of operation. When these active regions appeared on the Sun, we obtained

their images at a cadence of 10 s in high-resolution mode. The dark exposures are taken once a day after the observations were finished, just before closing the telescope. This is simply because the camera does not have any shutter. After closing the telescope shutter, no light enters the telescope and hence it becomes easy for obtaining the dark exposures. Flat-field images were taken once or twice a day during the observations. These images were taken by moving the telescope in all the possible directions by small amount. The daily observations were made in H_α line center at a cadence of 10 s. These images were sent to IIA, Bengaluru for further calibration and scientific analysis.

The H_α data needs to be processed before it is made useful for scientific analysis. The images are flat-fielded using the master flat. The following procedure is used to obtain the master flat. We obtained the shifted images while taking the observations. The telescope is shifted by about 10 pixels in random directions and about 10 to 12 images were obtained this way. The dark exposures were also taken and averaged to construct a master dark frame. Then the shifted images and master dark were used to make a master flat using the method described in [Chae \(2004\)](#). A sample master-flat image is shown in [Fig. 5\(left\)](#). The dust particles and other non-uniformity in the data can be seen in the flat. [Figure 5\(right\)](#) shows the flat-fielded image.

3.1 Image co-alignment

The obtained images were co-aligned with the first image in the time series. This was done by finding the correlation after shifting the images in the X and Y directions. The images were then co-aligned with the sub-pixel accuracy with the first image in the time series. Later, we co-aligned these images with the white-light image taken by Solar Dynamics Observatory. While aligning the image we made sure that the timings of the images in H_α and white-light are the same. These co-aligned images are useful for studying multi-wavelength nature of the transient events.

4. Preliminary data and results

Global Oscillation Network Group (GONG; [Harvey et al. 1988](#)) has updated its optics in 2010 to provide the H_α images to the solar community ([Harvey et al. 2011](#)). GONG uses 7-cm objective lens and its pixel resolution is 1''. It obtains the H_α images in all the 6 stations. [Figure 6](#) shows the comparison of GONG (Udaipur) and Merak H_α images. Obviously, Merak image has

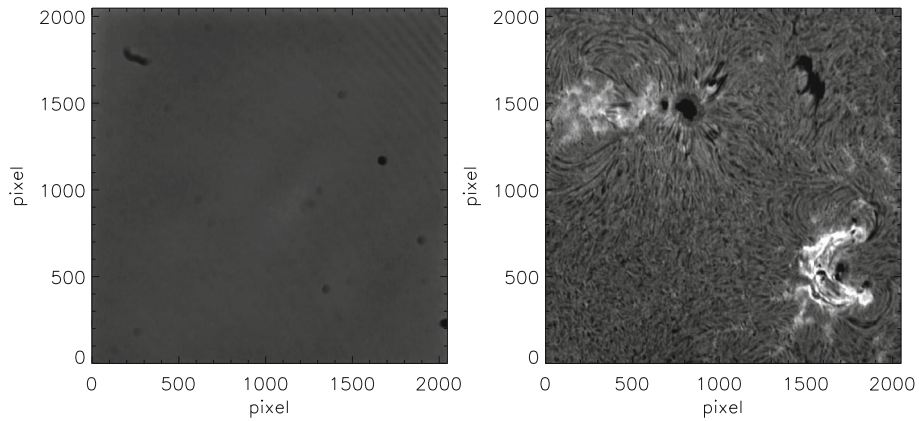


Figure 5. *Left:* Image obtained is master flat after using the method described in Chae (2004). *Right:* The dark subtracted and flat-fielded H_{α} image obtained on September 05, 2017 at 05:46 UT. The image field-of-view is $9.2'$.

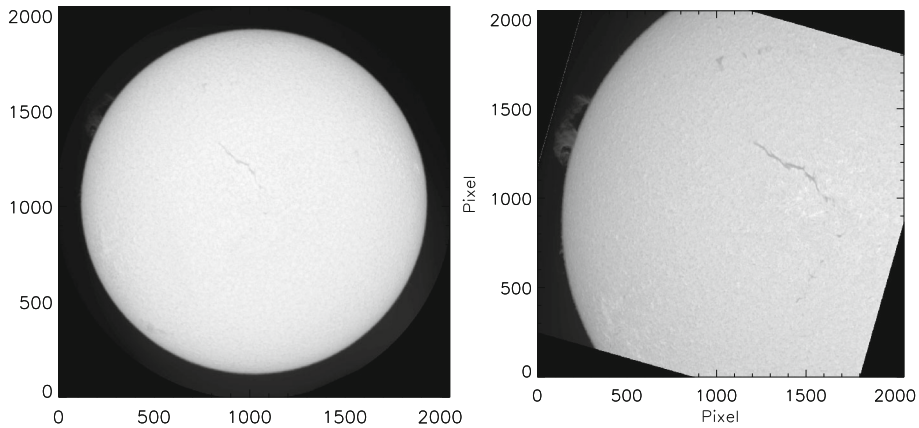


Figure 6. *Left:* The GONG H_{α} image obtained from Udaipur station on 19 October 2017. *Right:* The H_{α} image obtained from Merak site on the same day and close in time to the GONG image. The pixel resolution of the GONG image is about $1''$ and the Merak image is $0.68''$.

smaller FoV (with a pixel resolution of $0.68''$) because of the small format CCD camera. In both the images, it is easy to identify the filaments and plage regions. In the Merak image, the large prominence on the limb is clearly seen while it is barely visible in the GONG image. Apart from the large filament structure (which is lying in the East–West direction), there is one more filament below it lying in the North–South direction. Again, this is clearly seen in the Merak H_{α} image but not unambiguous in the GONG image. There is one more quiet Sun filament which is lying horizontally in the Northern hemisphere at high latitude, but not seen clearly in the GONG image. For this event, we did not have any observations from the Kodaikanal Observatory to make any meaningful comparison with its counterpart at Merak.

The active regions NOAA 12673 and 12674 appeared in the Southern and Northern hemispheres respectively, during the declining phase of the solar cycle 24. On September 05, 2017, both active regions crossed the

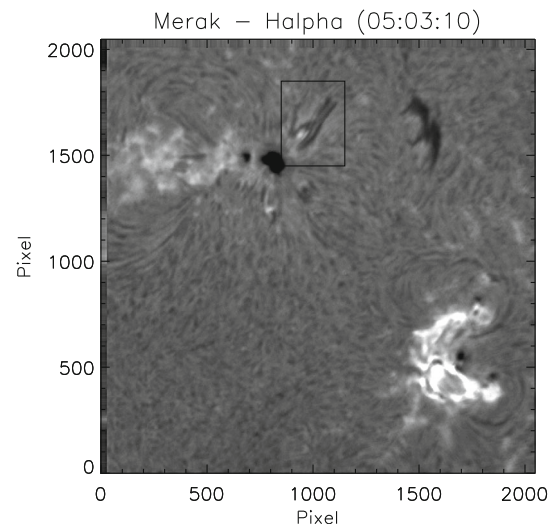


Figure 7. An image of the two active regions, filament and fibrils surrounding the sunspots are shown. A surge is shown by a boxed region near the active region NOAA 12674. The field-of-view of the image is $9.2'$.

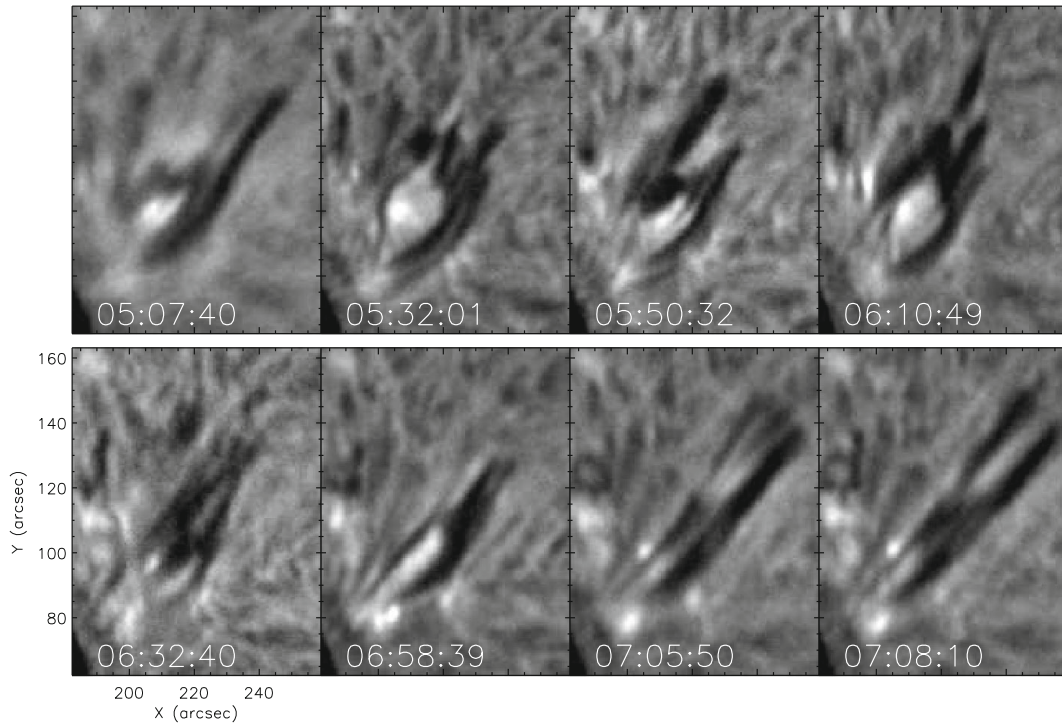


Figure 8. A time sequence of images showing the evolution of H_{α} surge.

central meridian passage. On September 06, 2017, the active region 12673 produced X9.3 class flare at 11:53 UT. On September 05, it produced several M and C class flares. The AR 12674 was little quiet compared to the other one. However, it has produced several surges during its lifetime. Figure 7 shows the location of the surge that occurred near the active region NOAA 12674. The surge location is shown in the boxed region.

Figure 8 shows a time sequence of H_{α} images extracted from the boxed region. The surge eruption was initiated at 03:10 UT. During the eruption phase (05:32 UT), it appeared as funnel-shaped and then it shrunk in width (06:32 UT). It elongated at 06:58 UT and erupted at 07:08 UT. Overall it took about 4 hours to erupt. The surge had bright ejecta surrounded by the dark ejecta in the funnel shape. A close look at the surge in the initial phase indicates that it is a filament and ejected as a surge.

Figure 9 shows a magnetogram of the same FoV as Fig. 7. The magnetogram is obtained from HMI instrument onboard the Solar Dynamics Observatory (SDO; Pesnell *et al.* 2012). The boxed region shows the surge location. Clearly the leading sunspot in AR 12674 is of negative polarity and the surrounding region is dominated by moving magnetic features with mixed polarity (MMFs; Harvey & Harvey 1973). Figure 10 shows the evolution of the magnetic fields in the surge location. Clearly, there is a collision of southern polarity

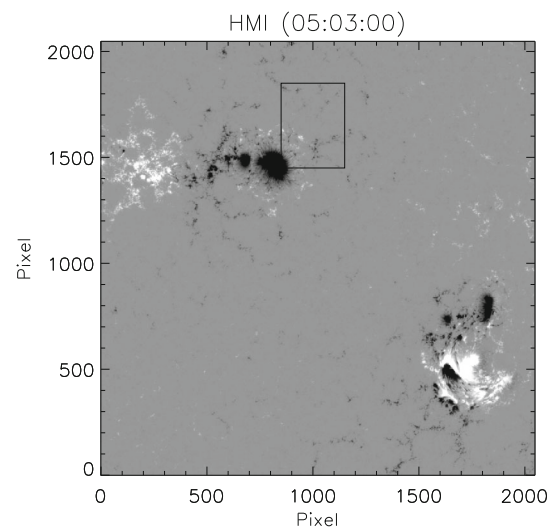


Figure 9. The image of magnetogram corresponding to the same field-of-view as H_{α} image shown in Fig. 7. The boxed region shows the location of jet in magnetogram.

region with the large northern polarity region followed by cancellation. The surge gets erupted during the disappearance of the southern polarity region. A more detailed result from this event will be presented in a future publication.

Figure 11 depicts the surge event near the active region 12673 when it moved towards the limb on September 9, 2017 at 07:17 UT. The surge erupted

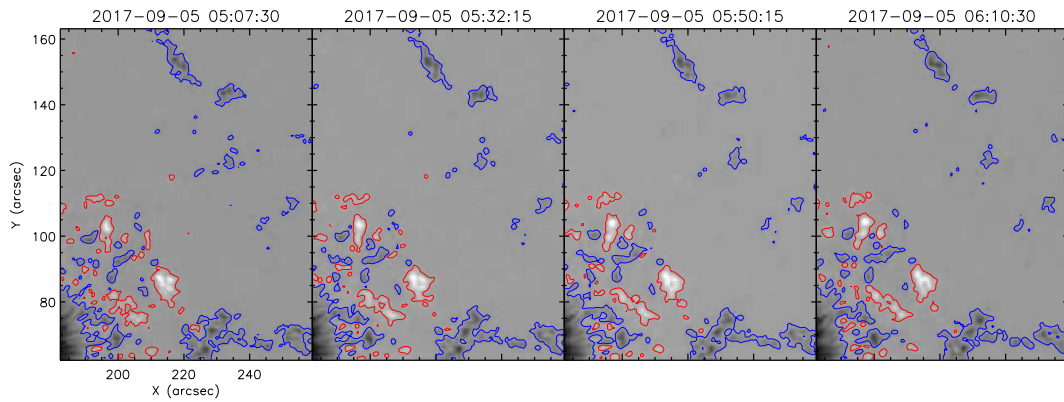


Figure 10. A time sequence of images showing the evolution of magnetic fields in the location of jet. The field-of-view is the same as Fig. 8.

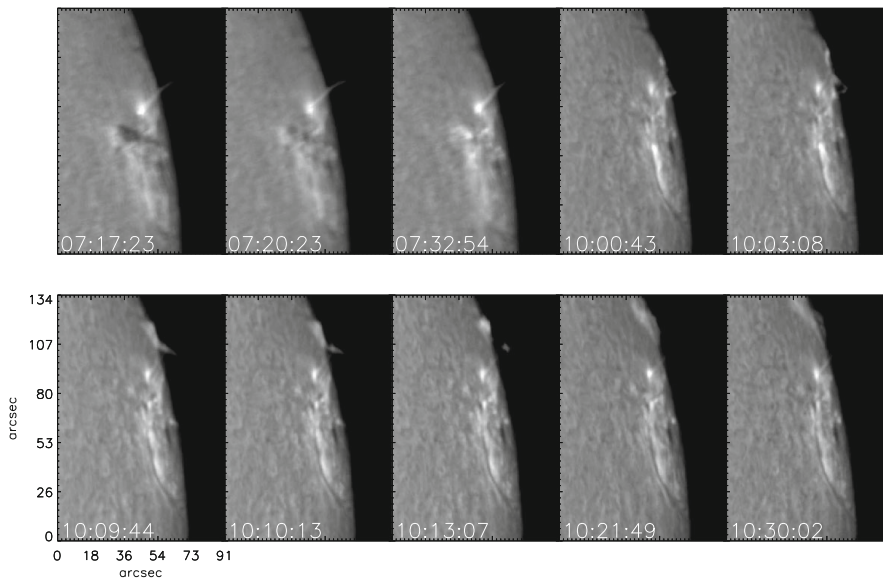


Figure 11. A time sequence of surge occurred in the limb near the AR 12673 observed on September 9, 2017.

in about half an hours time and several surges were frequently observed in that region. During our observation period, the region ejected 7 surges. Many of them were failed ones, they all fell back to the nearby prominence region.

5. Summary

Indian Institute of Astrophysics (IIA) has planned and designed the H_{α} telescope. Two identical telescopes were fabricated at NIAOT, China and tested for its performance. The NIAOT made 2 Lyot filters whose passbands were 0.4 \AA and 0.5 \AA . A team from NIAOT installed one of the telescopes at the Kodaikanal Solar Observatory in 2014 to continue the observations in the H_{α} wavelength which was initiated in 1912 at Kodaikanal. The Lyot filter installed at Kodaikanal has

a passband of 0.4 \AA . The second one was installed at the Merak site by IIA team, near the Lake shore of Pangong Tso, where IIA is planning to setup a large 2-m class telescope dedicated for solar observations. The H_{α} telescope was installed at Merak site in August 30, 2017. Since, then it is making the observations of the Sun whenever the sky is clear. The passband of the Lyot filter installed at Merak is 0.5 \AA . The chromospheric images obtained from the telescope showed fine features in the H_{α} wavelength and showed several surges in many active regions. The H_{α} telescope installed at Merak site provides another addition to the existing solar facilities at Kodaikanal.

The Lyot filter has the facility to tune it to any position on the H_{α} line profile. A stepper motor attached to the filter unit can be tuned to any point on the line profile with an accuracy of 10 mÅ. The tuning takes about 1 s to move the central passband from one position to the

other on the line profile. This property of the filter can be used to reconstruct the line profile and also can be used to find the Doppler shift in the line profile position. Using this, it is possible to make dopplergrams at the chromospheric heights (Dhara *et al.* 2016; Chae *et al.* 2006; Joshi *et al.* 2013). In future, we will produce such dopplergrams and make it available for scientific use.

At present, a smaller size CCD camera was used. This covers only 9.2' FoV. In future, we would like to replace it with a large format CCD to cover the entire 32' FoV. The Merak H α telescope is a new addition to the existing facilities at the Indian subcontinent. This trans Himalayan region largely remains unaffected by regular monsoon and thus enable useful and uninterrupted observations of the Sun.

Acknowledgements

The authors would like to thank Prof. Jadev Singh for initiating the H-alpha telescope program in IIA. The telescope and H α filter were fabricated and tested at Nanjing Institute for Astronomical Optics (NIAOT), CAS China. They thank the telescope team at NIAOT for their help and support. Special thanks to Prof. Weijun Mao for his constant encouragement and support during the development of the control software for the telescope at IIA. They would also like to thank the team members at IIA for their help during the installation of the telescope: B. Nagaraj, J. Manoharan, Tundup Stanzin, Tsewang Punchok, Tundup Thinless, Stanzin Norbo, Kunzhang Paljor, Konchok Nima, M. V. Ramaswamy, R. Ramachandra Reddy, Srinivasa, D. Parthiban, Vinay Kumar Gond, B. Pandiyarajan, Anand, Periyannayagam, Francis, Ramesh, P. R. Sreeramulu Nayak, Manjunath, Rajkumar and A. Mahendran. Without their help, it would not have been possible to install the telescope during those difficult conditions. Thanks are also due to the Director of IIA, Dr. Sree Kumar and Prof. Rangarajan for their constant support and encouragement during the testing phase of the telescope at Hosakote and installation of the telescope at Merak. They also thank the referees for their valuable comments which improved the manuscript.

References

Bethge C., Peter H., Kentischer T. J. *et al.* 2011, *Astron. Astrophys.*, 534, A105
Chae J. 2004, *Solar Phys.*, 221, 1

Chae J., Park Y.-D., Park H.-M., 2006, *Solar Phys.*, 234, 115
Denker C., Johannesson A., Marquette W., Goode P. R., Wang H., Zirin H., 1999, *Solar Phys.*, 184, 87
Dhara S. K., Ravindra B., Banyal R. K. 2016, *RAA*, 16, 10
Hagino M., Ichimoto K., Kimura G. *et al.* 2014, *SPIE*, 9151, 5
Harvey K., Harvey J. 1973, *Solar Phys.*, 28, 61
Harvey J. W., Hill F., Kennedy J. R., Leibacher J. W., Livingston W. C. 1988, *Adv. Space Res.* 8, 117
Harvey J. W., Bolding J., Clark R., Hauth D. *et al.* 2011, *SPD*, 42, 1745
Hale G. E., Ellerman F. 1906, *ApJ*, 23, 54
Hasan S. S., Soltau D., Krcher H., SüB M., Berkefeld T. 2010, *Astron. Nachr.*, 331, 628
Hasan S. S. 2012, *ASPC*, 463, 395
Hill F., Harvey J. W., Luis G. *et al.* 2009, in: *AAS/Solar Physics Division Meeting*, Volume 40, p. 845
Joshi Anand D., Srivastava Nandita, Mathew Shibu K., Martin Sara F. 2013, *Solar Phys.*, 288, 191
Labrosse N., Heinzel P., Vial J. C. *et al.* 2010, *Space Sci. Rev.*, 151, 243
Lin Y., Engvold O. R., Wiik J. E. 2003, *Solar Phys.*, 216, 109
Mackay D. H., Karpen J. T., Ballester J. L., Schmieder B., Aulanier G. 2010, *Space Sci. Rev.*, 151, 333
Otruba W., Potzi W., 2003, *Hvar, Obs. Bull.*, 2003, 27, 189
Pesnell W. D., Thompson B. J., Chamberlin P. C. 2012, *Solar Phys.* 275, 3
Prabhu K., Ravindra B., Hegde M., Doddamani V. H. 2018, *Astrophys. Space Sci.*, 363, 108
Qiu J., Wang H., Cheng C. Z., Gary D. E. 2004, *ApJ*, 604, 900
Ravindra B., Priya T. G., Amareswari K., Priyal M., Nazia A. A., Banerjee D. 2013, *Astron. Astrophys.*, 550, 19
Ravindra B., Prabhu K., Rangarajan K. E., Bagare S., Singh J., Kemkar M. M., Lancelot P., Thulasidharen K. C., Gabriel F. Selvendran R., 2016, *RAA*, 16, 127
Reda I., Andreas A. 2008, *NREL Technical Report*, NREL/TP-560-34302
Scherrer P. H., Bogart R. S., Bush R. I., Hoeksema J. T. *et al.* 1995, *Solar Phys.* 162, 129.
Scherrer P. H., Schou J., Bush R. I., Kosovichev A. G. *et al.* 2012, *Solar Phys.* 275, 207
Srivastava N., Ambastha A., Bhatnagar A. 1991, *Solar Phys.*, 133, 339
Stix M. 2002, *Second edition*, Springer Verlag
Tomczyk S., Mathew S. K., Gallagher D. 2016, *JGR*, 121, 6184
Vemareddy P., Maurya R. A., Ambastha, A. 2012, *Solar Phys.*, 277, 337
Verma V. K., Uddin W., Gaur V. P. 1997, in: *IAU Joint Discussion*, p. 19
Woodard M. F., Chae J. 1999, *Solar Phys.*, 184, 239
Zirin H., Liggett M., Patterson A. 1982, *Solar Phys.*, 76, 387
Zirker J. B., Engvold O., Martin S. F. 1998, *Nature*, 396, 440